Chemical and Biological Profile of Dual Cdk1 and Cdk2 Inhibitors

Stephan Ruetz[1], Doriano Fabbro[1,*], Juerg Zimmermann[1], Thomas Meyer[1] and Nathanael Gray[2]

[1]*Novartis Pharma Inc., Department of Oncology, CH-4002 Basel, Switzerland and* [2]*Genomics Institute of the Novartis Research Foundation, 10675 John Jay Hopkins Drive, San Diego CA, 92121, USA*

Abstract: The importance of Cdks in cell cycle regulation, their interaction with oncogenes and tumor suppressors, and their frequent deregulation in human tumors, has encouraged an active search for agents capable of perturbing the function of Cdks. In our laboratories, a variety of selective and potent low molecular weight inhibitors directed against the ATP binding sites of the Cdk1, Cdk2 have been developed. Extensive biological profiling of two distinct classes of Cdk inhibitors – the phenylamino pyrimidines (PAPs) and trisubstituted purines has revealed distinct differences in their cellular effects in normal cells compared to tumor cells. Due to their intact G1/S checkpoints, normal cells are shown to be reversibly blocked by these Cdk inhibitors in either the G1/S-phase or at the G2/M boarder. In transformed cells these control points are either absent or defective and treatment with the compounds resulted in pronounced proliferation block at the G2/M transition. Furthermore, there is strong evidence that this G2/M arrest is less well tolerated by the cells and consequently, they undergo apoptotic cell death. Finally, these dual Cdk1/ Cdk2 inhibitors are also found to be significantly more active on proliferating cells compared to quiescent cells reflecting their specific activity. Despite these encouraging results demonstrating a distinct outcome after treatment with such dual Cdk inhibitors in normal compared to de-regulated tumor cells, it remains to be determined whether a comparable therapeutic window might be observed *in vivo* experiments. Furthermore the intracellular kinase selectivity of inhibitors which are putatively selective *in vitro* remains a complicating feature that is only recently begun to be addressed by affinity chromatography and phosphoproteomics techniques. Once efficacy can be demonstrated in animal models at well-tolerated doses, there will be strong evidence for the development of cell cycle antagonists for cancer therapy.

1. TARGETING CYCLIN-DEPENDENT KINASES CDK 1 AND CDK2

Cell cycle progression in normal eukaryotic cells is triggered and strictly regulated by a family of closely related cyclin-dependent kinases (Cdks) [1-5]. Different activated enzyme complexes of these Cdks control the transition between the distinct cell cycle phases. Due to their importance in the coordination of different cell cycle events, the kinase activity of these enzymes are tightly regulated. In a majority of human tumors, Cdk activity is frequently deregulated or the Cdk complexes interact with oncogenes and/or tumor suppressors which results in the loss of fidelity of mechanisms and pathway that replicate, repair, and segregate the genome [1,3,4,6-8,9].

In addition, in many cancers mutations in the retinoblastoma protein gene (pRb) itself have been found to affect its tumor suppressor function at the critical G1/S transition point of the cell cycle. This checkpoint is normally orchestrated by Cdk2 activity, and thus, an inhibitor directed against the G1-regulating Cdk activities would not arrest cells at G1 border [10, 11]. Based on these observations and the fact that the catalytic units of the Cdk1 and Cdk2 proteins are very similar, in particular around the ATP binding site, we sought to develop potent and selective inhibitors that block the protein kinase activities of both enzymes. This review focuses on the medicinal chemistry and enzymatic and cellular characterization of two different compound classes, the phenyl-amino-pyrimidines and the trisubstituted purines. In addition, data from selected experiments are presented testing the hypothesis that dual inhibition of Cdk1/2 will result in different cellular phenotypes dependent on the functionality of the tumor suppressor protein pRB. According to this hypothesis, cancer cells with defective pRb would override the G1/S checkpoint and eventually arrest at the G2/M transition point due to the Cdk1 inhibition. In contrast, a dual Cdk1 and Cdk2 inhibitor should arrest normal cells reversibly either at the G1/S (in the case of a functional pRb) and/or at the G2/M transition. In addition, the selected experiments address the important question whether cells arrested at G2/M boarder either apoptose or undergo endoreduplication (i.e. re-enter S without M) and then eventually die by apoptosis.

2. CGP60474: A DUAL INHIBITOR OF CDK1 AND CDK2 KINASE ACTIVITY

Various inhibitors against the protein kinase activities of Cdk1 and Cdk2 have been identified [12-16]. Initially, in the search for new chemical structures capable of inhibiting protein kinase C (PKC), we identified a series of phenyl-amino-pyrimidines (PAPs) which turned out to be very versatile and could be used to design inhibitors of various protein kinases, including Cdk1 and Cdk2 [17,18]. Starting from a phenylamino pyrimidine lead, a medicinal chemistry effort resulted in the identification of a low nanomolar Cdk inhibitor which was named CGP60474 (Fig. **1**). Docking

*Address correspondence to this author at the Novartis Pharma Inc. Department of Oncology, WKL-125.4.10, CH-4002 Basel, Switzerland; Tel: +41 61 696 7681; Fax: +41 61 696 3835;
E-mail: doriano.fabbro@pharma.novartis.com

1568-0118/03 $41.00+.00

studies and analysis of the structure-activity relationships support a binding mode where CGP60474 adopts the usual bidentate hydrogen binding mode: the pyrimidine-N1 with the amide-NH of L83 and the anilino NH with the carbonyl group of L83, while the N6-amino group in ATP donates a hydrogen to the backbone carbonyl of E81 (Fig. **1**).

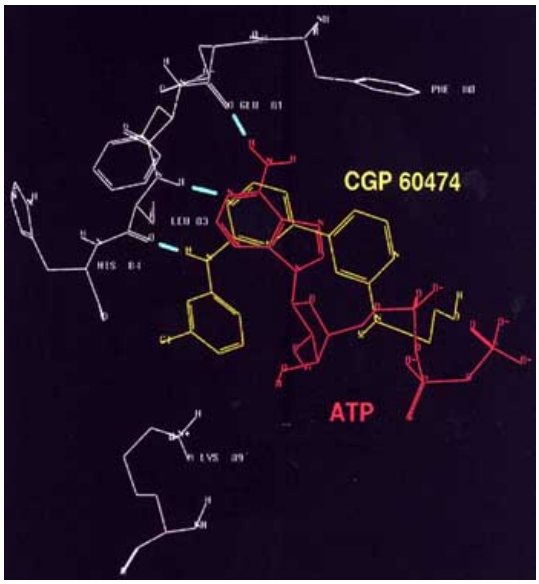

Fig. (1). Mode of binding of CGP60474 to the hinge region of Cdk2.

Binding of CGP60474 to the hinge region of Cdk2. Bi-dentate binding mode of CGP60474 docked to the ATP binding site of Cdk2 as described [43]. H-bonds are in blue. Expression, purification and enzyme assays for the various kinases were performed as described [44].

2.1. *In Vitro* Profile of CGP60474

Despite using the highly conserved hinge region as a key recognition feature for H-bonding interactions, CGP60474 displays a remarkable kinase selectivity profile *in vitro*. CGP60474 inhibits Cdk1/cyclinB and Cdk2/cyclinA with IC_{50} values of 17 and 80 nM respectively which are at least 10 to 50 fold lower than the activity of the compounds against the next related kinase, Cdk4. Of the kinases tested, CGP60474 displayed only marginal inhibition of PKC-α and v-Abl with IC_{50} values in the 250 to 400 nM range. The remaining kinases were not significantly inhibited by CGP60474 (Table **1**).

The anti-proliferative effect of CGP60474 was tested in a broad panel of established tumor cells derived from different origins. Strikingly, in most cell lines the compound was very effective in inhibiting cell growth in the low nanomolar range (Table **2**). Only in a few cases were IC_{50}s greater than 100 nM observed (Table **2**). Treatment of normal human fibroblast cell line WI-38 with CGP60474 resulted in inhibition of phosphorylation of pRB Since pRB is a known downstream target of Cdk2 and this last phosphorylation step from the hypo- to the hyper form is only mediated by active

Table 1. Effect of CGP60474 on the Activity of Purified Protein Kinases (IC_{50} Values in nM) and on Tyrosine Phosphorylation Induced by EGF, PDGF-BB and SCF in Intact Cells

Enzyme	IC_{50} (nM)	Enzyme	IC_{50} (nM)
Cdk1/cycB ATP)	17	EGF-ICD	9'700
Cdk2/cycA	80	v-Abl	400
Cdk2/cycE	50	GST-Kdr	> 1'000
Cdk4/cycD1	700	c-Src	11'100
PKC-α	250	Flt1	1'000
PKC-βI	4'200	Tek	> 1'000
PKC-βII	1'900	c-Met	5'700
PKC-γ	2'300		
PKC-δ	24'000	**Target molecule**	**IC_{50} (nM)**
PKC-ε	17'300	PDGF-R	> 100'000
PKC-ζ	> 100'000	EGF-R	> 100'000
PKC-η	5'700	c-kit	1'000 – 3'000
PKA	160'000		

Enzyme assays were performed as described in (). Serial dilutions were done in duplicates or triplicates with SD ± 10%. Data (IC_{50}s; nM) represent mean values of at least two independent experiments. Mean variation between individual experiments was in the range of ± 40 % to ± 70 %. Cellular ELISAs were used to monitor the effects of the compounds on total tyrosine phosphorylation of the platelet derived growth factor receptor (PDGF-R) and epidermal growth factor receptor (EGF-R) measured by anti-phosphotyrosine antibodies after stimulation of Balb/c 3T3 cells with 50 ng/ml of (PDGF-BB) or A431 cells with 100 ng/ml of (EGF), respectively as described in (). Mo-7e cells were incubated for 24 h in the presence of 50 ng/ml stem cell factor (SCF) to activate c-Kit. The degree of phosphorylation was measured in cell lysates. Data represents means values of two independent experiments.

Cdk2 kinase activity, these data confirmed that CGP60474 is capable of inhibiting intracellular Cdk2 activity. Consistent with this observation, Cdk2 kinase activity immunoprecipitated from total cell lysates demonstrated that CGP60474 abolished this activity in a dose-dependent manner.

2.2. Cellular Profile of CGP60474

2.2.1. Inhibition of Cell Proliferation by CGP60474

Encouraged by the enzymatic and cellular profile of CGP60474, extensive characterization of the cellular activity of the lead compound CGP60474 was performed. Initially, we intended to test the hypothesis that cancer cell lines with a defective G1/S checkpoint due to inactivated pRb protein are indeed more sensitive to a dual Cdk1/2 inhibitor than cells with a functional pRB pathway. For these experiments we selected a pair of osteosarcoma cell lines, U2OS and U2OS/Tag. The latter subline was established by stable transfection of U2OS cells with a construct carrying the full-length cDNA of the large T antigen known to bind the pRB protein and inactivate its function during the G1/S transition. As shown in Fig. (**2**) (right panels), treatment of U2OS and U2OS/Tag cells with increasing concentrations of CGP60474 caused a time-dependent growth arrest in both

Table 2. ***In Vitro*** **Antiproliferative Effect of CGP60474 on Tumor Cells (IC_{50} Values in nM)**

Cell line	IC_{50} (nM)	Cell line	IC_{50} (nM)
Colon		**Prostate**	
DLD-1	34	DU-145	20
HTC-15	84	PC-3	17
HTC-116	32	**Ovary**	
Colo 205	25	PA-1	18
Breast		SW-626	69
MDA-MB-453	280	ES-2	38
MDA-MB-231	21	**Others**	
MDA-MB-468	75	A431	24
BT-20	40	T24	36
ZR-75-1	100	A31	120
MCF-7	70	A-498	66
Lung		Caki-1	22
A549	40	Balb/c c-sis	81
NCI-H596	68	KB-8511	28

Antiproliferative *in vitro* assays were performed in 96-well microtiter plates. Cells were seeded as indicated and incubated overnight. Compounds were added in serial dilutions on day 1 and cells incubated for additional 3 to 5 days allowing control cultures to undergo at least 3 cell divisions. After incubation cells were fixed with 3 % v/v glutaraldehyde, washed with water and stained with 0.05 % methylene blue. After washing, the dye was eluted with 3 % v/v HCl and the optical density measured at 665 nm either as described in Methods. IC_{50}s were determined by a computerized system using the formula (OD test - OD start) / (OD control - OD start) x 100. Serial dilutions were done in duplicates or triplicates with SD ± 10 %. IC_{50}s represent mean values of at least two independent experiments. Mean variation between individual experiments was 30 % - 50 %.

cell lines. This antiproliferative effect was remarkably dose-dependent but quite similar in both cell lines with IC_{50} values of 95 nM for U2OS/Tag and 115 nM for U2OS cells. However, in contrast to U2OS cells, a significantly higher portion of the U2OS/Tag cells showed impaired viability and underwent apoptotic cell death. This effect increased over time reaching levels of over 50 % of affected cells and showed a clear concentration dependency (Fig. **2**, left panels). Thus, although CGP60474 has comparable antiproliferative activity in cells with functional pRB and cells with a deficient G1/S transition checkpoint, the consequences on cellular viability are quite different.

2.2.2. Cell Cycle Analysis of Cells Treated with CGP60474

To further elucidate the molecular mode of action of CGP60474, cell cycle progression was assessed by flow cytometry analysis (FCM) in U2OS and U2OS/Tag treated for 24, 48 and 120 hours with increasing concentrations of the inhibitor. As shown in Fig. (**3**), an increase in the G1 cell population was observed in U2OS control cells. As a consequence, there was a significant reduction of the number of cells in S- and G2/M-phase presumably because CGP60474 mainly targeted Cdk2 kinase activity. This G1/S block seemed to be well tolerated by the cells since only a minor portion of apoptotic subG1 cells appeared in the FCM profile. In contrast, in U2OS/Tag cells CGP60474 caused an accumulation of arrested cells in G2/M, presumably as a result of activity against Cdk1. Consistent with the previous results, an increase of a subG1 population of cells representing apoptotic cells was observed. That latter effect again showed a clear time- as well as dose-dependency. These data suggested that the dual Cdk inhibitor CGP60474 indeed acts differently in cells with an intact G1/S transition checkpoint compared to cells with inactive pRB protein. In addition, these data support the hypothesis that a G1/S block is relative well tolerated by the cell while cells blocked at the G2/M border eventually undergo cell death.

2.2.3. Preferential Killing of pRB Deficient Cells by CGP60474

Thus, it remained to be demonstrated that this dual mechanism of action of CGP60474 would translate into a therapeutic window due to a preferential G2/M arrest and onset of apoptosis in cells with mutant pRB protein question. To address this question, a mixed culture containing equal numbers of U2OS and U2OS/Tag cells were synchronized in G1/S with mimosine [19]. Once arrested in the G1 phase, mimosine was washed out and the cells were released into the cell cycle for 16 h in the absence or presence of 100 nM CGP60474. After treatment the inhibitor was removed by extensive washing and the culture was resuspended in normal growth medium for 96 hours. During that period, aliquots of untreated and CGP60474-treated cells were harvested every 24 hours and analyzed for expression of Cdk1 and large T antigen by immunostaining (Fig. **4**). Equal amounts of Cdk1 protein as well as the large T antigen were present in cells treated or not treated with CGP60474 and collected 16 hours after release from the mimosine block. In contrast, in the samples collected after the first 24 hours of the recovery phase, a remarkable change was observed. In the untreated cell population the expression of Cdk1 as well as the large T antigen protein was slightly increased consistent with an overall increased cell number in these samples. However following treatment with CGP60474 for 16 hours the level of Cdk1 and large T antigen was reduced. Since the latter protein is only expressed in U2OS/Tag cells, these findings suggested that a significant population of the U2OS/Tag underwent apoptotic degradation although it cannot be excluded that also normal U2OS cells died. However, analysis of treated aliquots collected after 48 hours, 72 and 96 hours revealed that the relative expression level of Cdk1 recovered indicating active proliferation while in the same aliquots the expression of the large T antigen decreased continuously. Thus, in these aliquots normal U2OS cells survived while the majority of the U2OS/Tag cells underwent apoptosis. The interpretation of this experiment is that the use of dual Cdk1 and Cdk2 inhibitors might open an opportunity to target specifically tumor cells with an impaired G1/S transition checkpoint.

2.2.4. CGP60474 Inhibits Proliferatin of Cycling Cells Only

We next investigate whether CGP60474 also affects the viability of quiescent cells. As Cdks are predominantly activated during cellular proliferation one might expect that a specific inhibitor should well be tolerated in non-

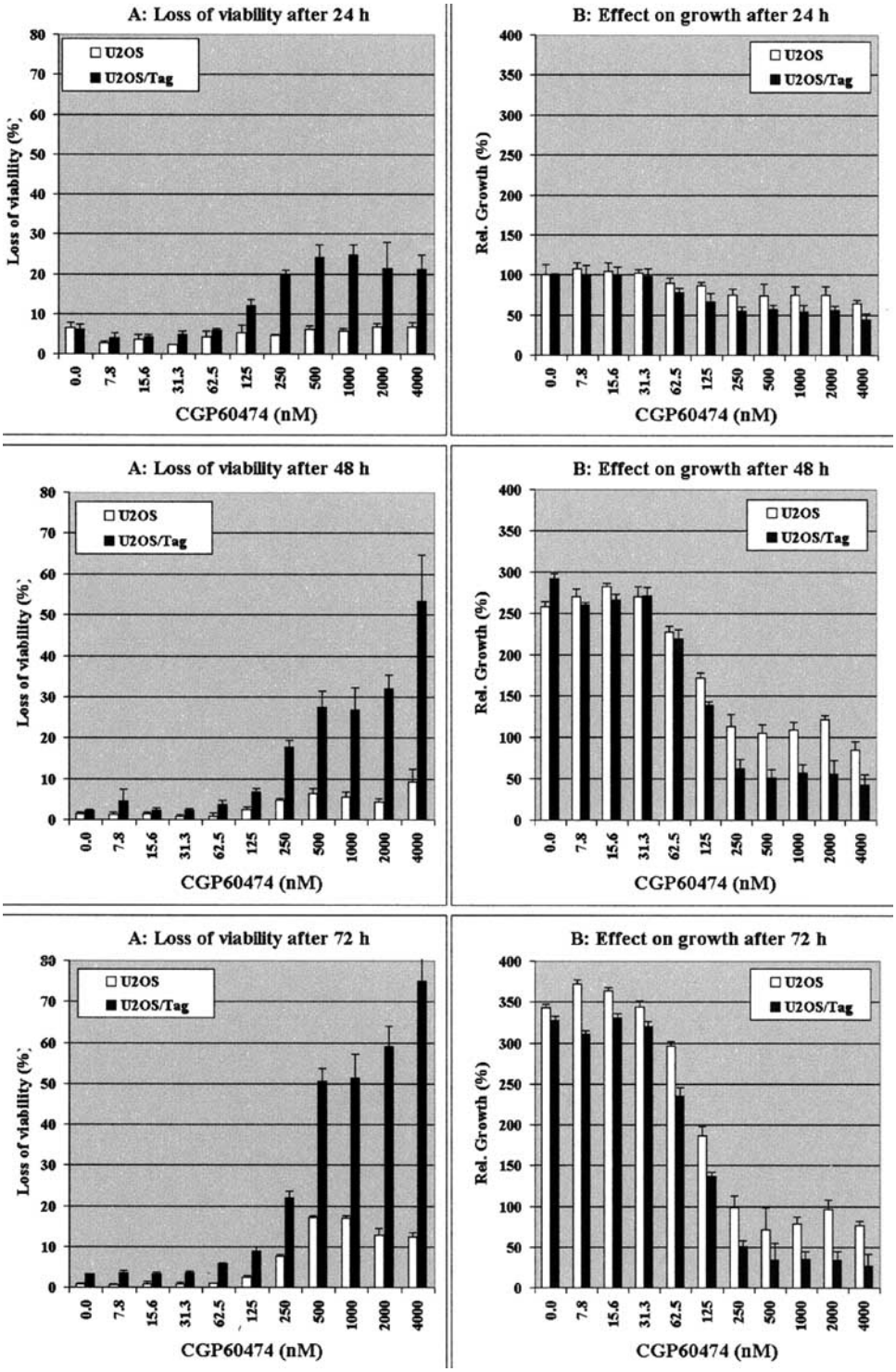

Fig. (2). Time-dependent effect on cell proliferation and loss of viability in U2OS and U2OS/Tag cells treated with increasing concentrations of CGP60474.

Exponentially growing cells were treated for 24 h, 48 h and 72 h with increasing concentrations of CGP60474. Induction of apoptosis (A) and effect on proliferation (B) was assessed using the DNA-interchalting dye YO-PRO-1 iodide [45]. Data represents means values of triplicates of at least two independent experiments.

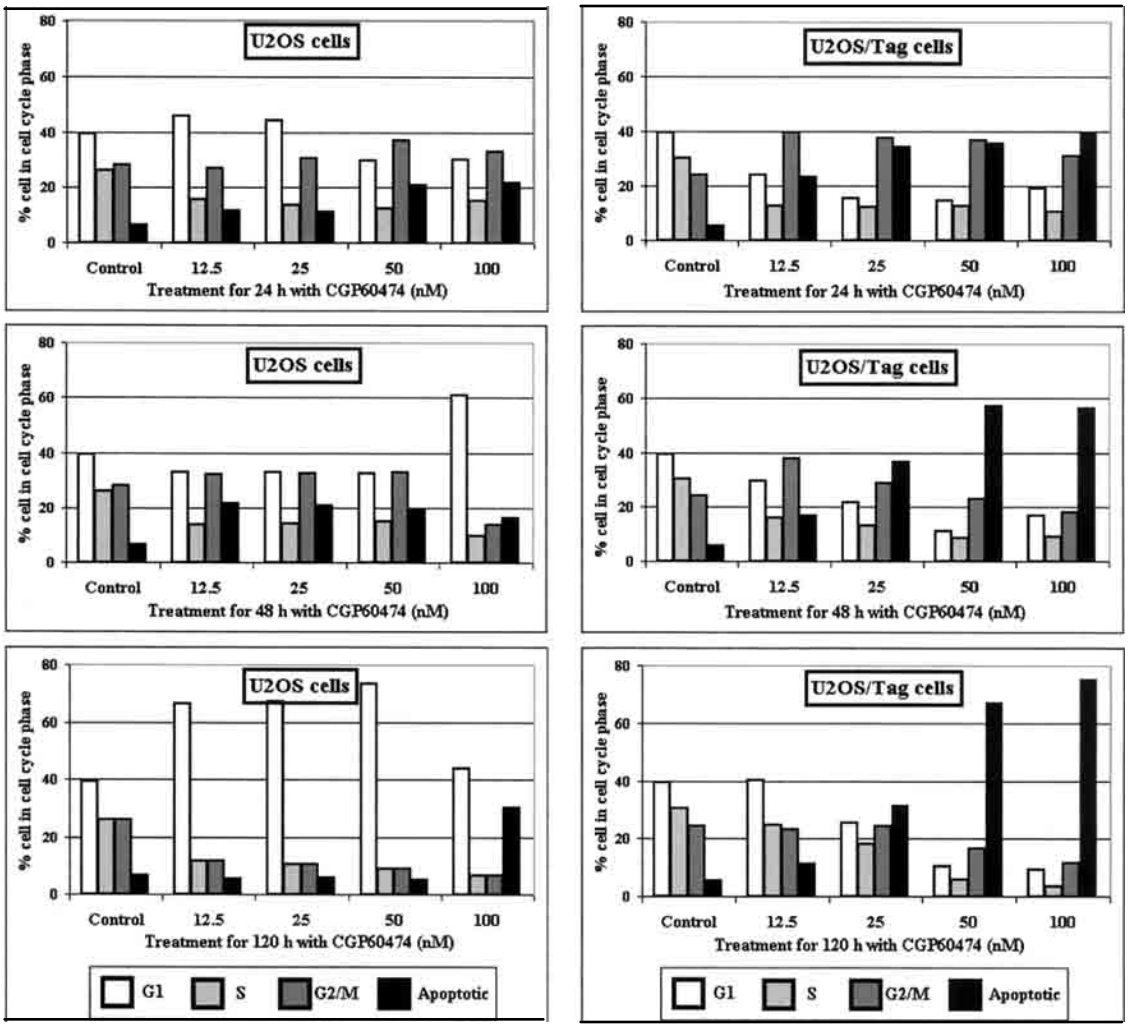

Fig. (3). Dose and time-dependent arrest in specific cell cycle phases in U2OS and U2OS/Tag cells treated with increasing concentrations of CGP60474.

Exponentially growing cells were treated for 24 h, 48 h and 120 h with increasing concentrations of CGP60474. Cell populations arrested in the different phases of the cell cycle were assessed by standard flow cytometry (FCM) analysis and quantified using standard protocols.

proliferating cells. For these experiments we took advantage of the human fibroblast cell line WI-38, which are known to divide in tissue culture for only a limited number of passages after which they start to differentiate. We treated such senescent cells as well as exponentially proliferating WI-38 cells with increasing concentration of CGP60474 for 48 h and 120 h and scored for loss of viability. In addition, we included in these experiments the SV-40 transformed subline WI-38/VA (Tag) with a dysfunctional pRB pathway. As shown in Fig. (**5**), in both normal cell lines the compound showed only minor effects after 48 h. However, in WI-38/VA(Tag) cells with an impaired G1/S transition checkpoint again a dose-dependent increase of an apoptotic cell population was observed. Setting a threshold value of 25 % apoptotic cells, these latter cells reached this level at a drug concentration of 500 nM. After 120 h treatment (B), we also observed a dose-dependent appearance of apoptotic cells in the control lines. In the proliferating WI-38 cells the 25 % threshold value for apoptotic cells was crossed at 250 nM and in the quiescent line at about 750 nM. In contrast, the viability of WI-38/VA (Tag) cells was already significantly affected at a concentration of 50 to 60 nM CGP60474. Taken together, although unspecific activity of CGP60474 cannot be excluded, the compound is certainly more effective in proliferating cells. In addition, the findings with the WI-38/VA(Tag) subline further supports the hypothesis that cells with an mutated pRB pathway are more sensitive to treatment with dual Cdk inhibitors.

3. OPTIMIZATION OF OLOMOUCINE AS DUAL CDK INHIBITORS

3.1. Enzymatic Profile of Olomoucines

Although CGP60474 was a very potent inhibitor with a reasonable selectivity spectrum it had other unfavorable properties that precluded its further development. We

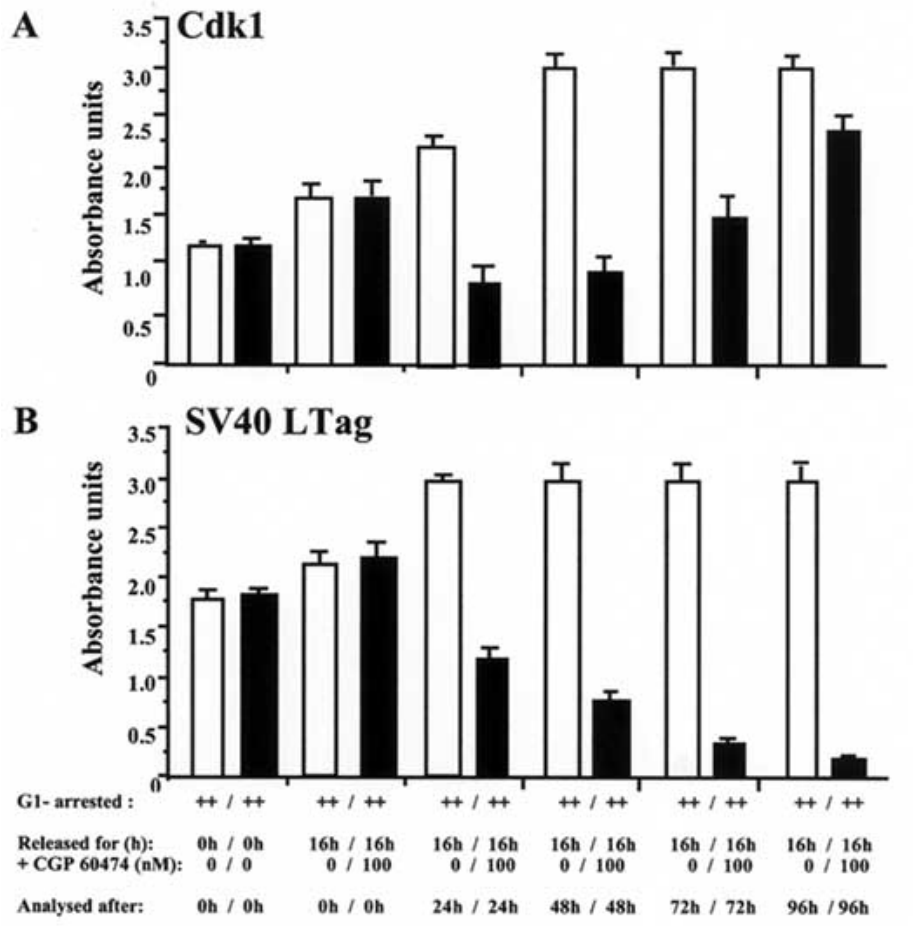

Fig. (4). Recovery of U2OS and U2OS/Tag cells after treatment with CGP60474.

Equal numbers of exponentially growing U2OS and U2OS/Tag cells were cultured together and synchronized with mimosine [19]. Once arrested in the G1 phase, mimosine was washed out and the mixed cell population released into the cell cycle for 16 h in the absence or presence of 100 nM CGP60474. After removal of the kinase the recovery from the treatment was assessed by maintaining the mixed cell population for 96 h in normal growth medium. During that period, every 24 h a defined aliquot of untreated and CGP60474 treated cells was harvested. After lysis, equal aliquots of each samples were spotted onto nitrocellulose in a dot-blot device. The membranes were incubated with a monoclonal anti-Cdk1 or anti-SV40 large T antigen antibody following standard protocols. The revealed staining of the two proteins was quantified by a density scans. Data represent means values of six scans of one of two independent experiments.

therefore optimized the purine derivative olomoucine, another promising scaffold with a reasonable selectivity for Cdk1 and Cdk2 [20]. Impetus for the development of purines as CDK inhibitors came from the discovery that olomoucine, a 2,6,9-trisubstituted purine previously known for its antimitotic activity, is an inhibitor of starfish-derived Cdk1/cyclin B [21]. Kinetic analysis suggested a mechanism of direct competition with ATP for binding to the kinase active site [22, 23]. Although olomoucine possessed a relatively weak inhibitory activity (IC_{50} on purified starfish cdc2/cyclin B of 7 μM) relative to the highly potent nonspecific inhibitor staurosporine, it appeared to be relatively selective when tested against a panel of kinases [24]. This was an important finding because there was much skepticism that any compound targeting the highly conserved ATP binding site could possess the requisite selectivity. Also in contrast to staurosporine, olomoucine was a structurally simple trisubstituted purine and was therefore easy to derivatize. The cocrystal structure of olomoucine bound to human Cdk2 revealed that although olomoucine occupies a region that mostly overlaps the ATP binding site, the 6-benzyl substituent extends into a region not occupied by ATP and presumably accounts for the selectivity of the inhibitor [24] (Fig. **6**). The purine ring of olomoucine is also rotated relative to that of ATP such that the H-bonds made to the kinase hinge region by exocyclic amino and N3 are replaced by the C6 NH and N7.

3.2. Optimization of Olomoucines by "Focused Libraries"

Not surprisingly, the discovery of olomoucine stimulated much interest in exploring purine and related heterocyclic scaffolds as inhibitors of Cdks and other kinases by both academic and pharmaceutical groups [25 - 27]. Structure activity studies performed using a combination of traditional medicinal chemistry approaches and combinatorial approaches resulted in the synthesis of compounds such as roscovitine [28] the purvalanols [29], bohemine, CVT 313

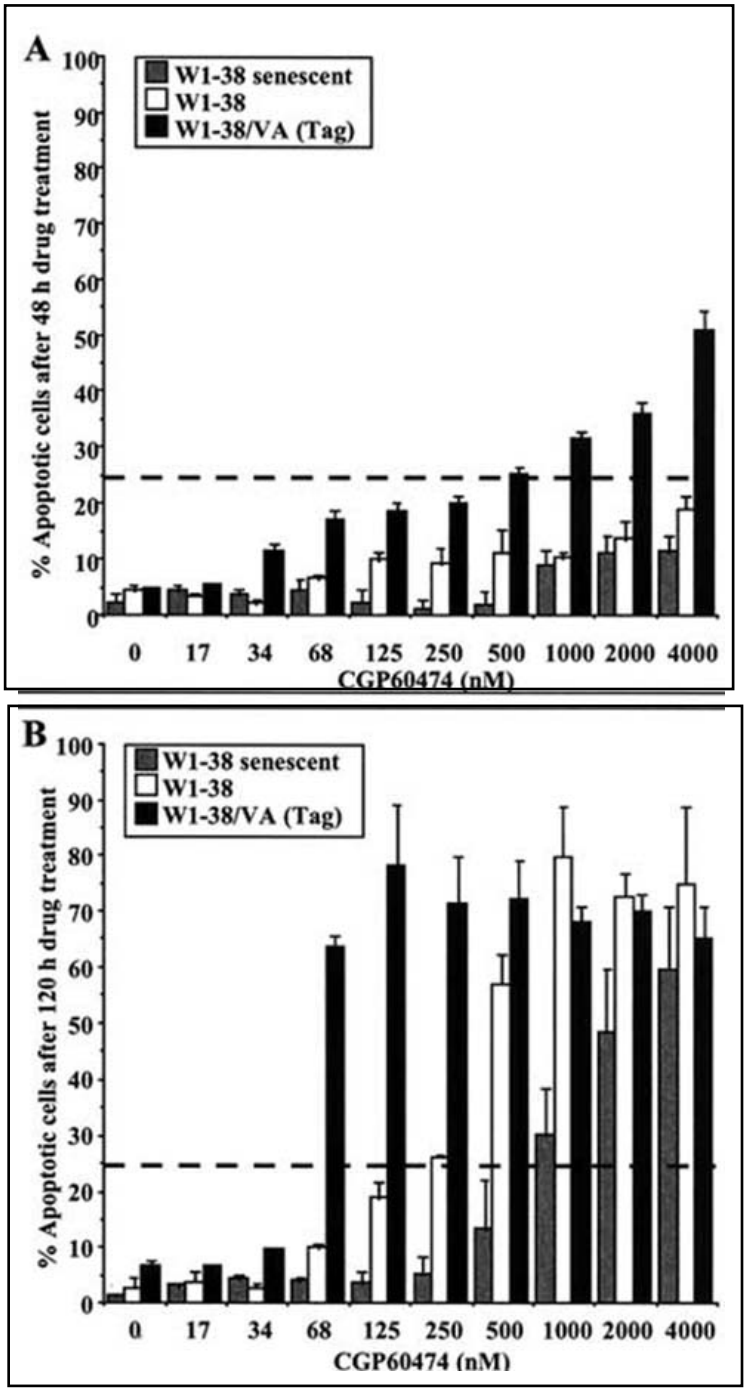

Fig. (5). Effect of CGP60474 on survival of proliferating WI-38 and SV40-transformed WI-38/VA cells and on senescent WI-38 cells.

Exponentially growing cells were treated for 48 h (A) and 96 h (B) with increasing concentrations of CGP60474. Loss of viability was assessed using the DNA-inter-chalting dye YO-PRO-1 iodide [45]. Data represents means values of triplicates of at least two independent experiments.

[30], CGP74514 [27], and H717 [31] (Fig. 7). Optimization efforts focused on finding trisubstituted purines of improved potency and selectivity against a panel of kinases that could be tested *in vitro*. Analysis of the Cdk2-olomoucine cocrystal structure revealed that: (1) the C2 substituent is directed into the ribose triphosphate binding site and can potentially tolerate large substitutions, (2) the C6 benzylamino substituent is directed into a hydrophobic pocket that

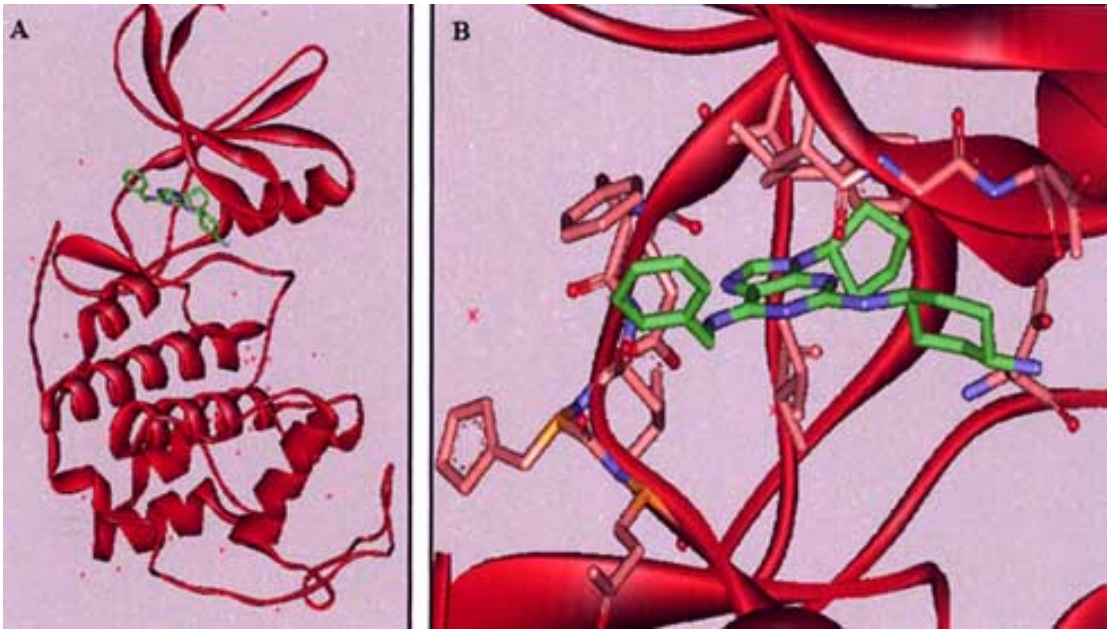

Fig. (6). Cocrystal structure of the trisubstituted purine H717 bound to Cdk2.

Ribbon diagram of Cdk2 showing H717 bound in the ATP-binding cleft located between the N and C-terminal lobes (A). Enlarged view of active site showing binding sites for C6-benzylamino substituent (located in "specificity pocket"), C2-cyclohexylamino (located in ribose-binding pocket), and N9-cyclopentyl (located in small hydrophobic pocket) (B).

ultimately opens to solvent, and (3) the N9 substituent faces a small hydrophobic pocket. In order to rapidly identify optimal substituents, two general library strategies were developed: "focused-libraries" where two of the three diversity sites were held fixed while many different substituents were tested at one site and "diverse libraries" where all three diversity sites were simultaneously varied. Providing that improvements in binding affinity at each of the three sites is independent of the others, the focused library approach is the most efficient method for exploring diversity at each site and incorporation of diversity at the final step of the synthetic scheme is optimal. In contrast, diverse libraries are appropriate when synergistic or antagonistic effects are expected between sites and possible alternate binding modes are sought. An excellent example of the value of exploring diverse trisubstituted purines is exemplified by the identification of 9-unsubstituted 2-amino substituted purines such as NU2058, one in a series of potent Cdk1/2 inhibitors developed by Astra Zeneca [32, 33]. These compounds differ from olomoucine-type compounds by binding to Cdks through hydrogen bonds between the amino and carbonyl group of Leu83 and the C2 amino and N3 nitrogen of NU2058, respectively. This sort of binding mode would never have been uncovered in a purely focused library effort based on an olomoucine-type lead.

An example of a solution and a solid phase scheme for the preparation of diverse purine libraries is shown in Fig. (**8**). The solution phase route starts with the introduction of a first diversity element by alkylation of a 2-fluoro or 2, 6-dichloropurine core scaffold. Amines (including primary, secondary and anilines) are then introduced sequentially at the C6 and C2 by displacement of the halo substituents (Fig. **8A**). This solution phase scheme is ideally suited for the production of focused libraries at C2 through the preparation of an advanced intermediate (*i.e.*, 2-fluoro-6-(3-chloro-anilino)-9-isopropylpurine) followed by introduction of different amines at C2. The solid-phase route starts by using a resin-bound amine to capture the alkylated purine followed by subsequent diversification at C2 using either palladium-mediated coupling reactions with anilines, phenols, or boronic acids or by direct nucleophilic displacement of the 2-fluoropurine with amines [34, 35] (Fig. **7B**).

The structure-activity relationships for trisubstituted purines against Cdk1/cyclin B starting from the olomoucine lead will be discussed in terms of the replacements that can be made to the C2, C6, and N9 positions (Fig. **9**). Replacement of olomoucine's C2- ethanolamino substituent with R-valinol results in a 3-6 fold improvement in IC_{50} (**118** vs **75** and **52** vs purvalanol A). In general, optimal C2-substituents consisted of alpha-branched and cycloamino alcohols. While changes in affinity resulting from substitutions at the 2, 6, and 9 positions were for the most part independent of one another, there were several exceptions. For example, replacement of a C2-ethanol with a piperidinylethanol in the context of a 6-(4-methoxybenzylamino) group (**118** vs **10**) resulted in a 3-fold improvement in activity, while the same C2 substitution in the context of a 6-(3-chloroanilino) (**52** vs **306**) resulted in a 6-fold loss of activity. Although the Cdk2-bound conformation of C2-piperidinylethanol-substituted purines has never been solved, it is likely that the 6-(3-chloroanilino) substituent cannot assume an optimal orientation in the presence of this substituent. A hydrogen-bond donor (NH) is not required at C2 as evidenced by the potent activity of

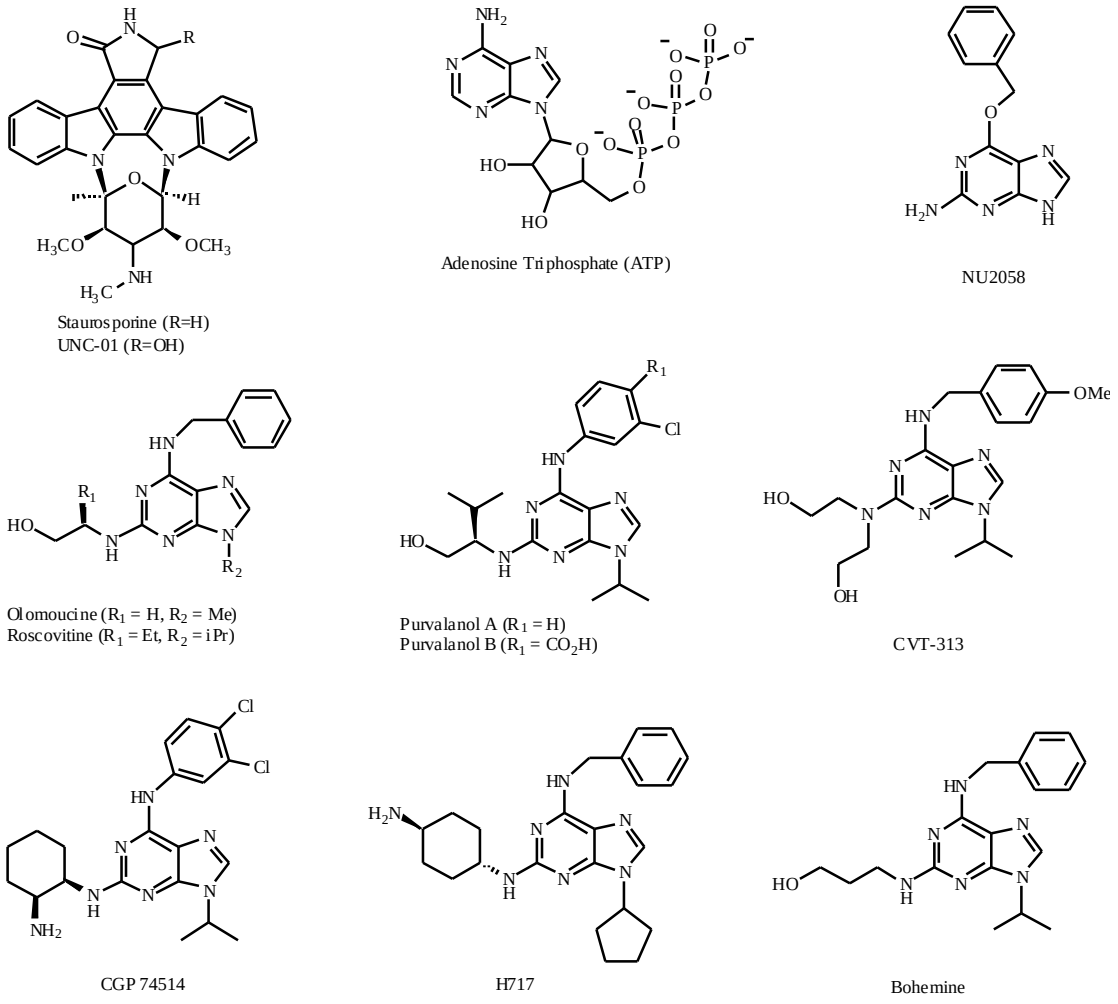

Fig. (7). Strucure of various ATP-site binding compounds.

compounds where this group is replaced with cyclic (**10**) or acyclic (**26**) secondary amines and alkynes (**2b**). The C6-benzylamino substituent tolerated substitution at the meta and para positions but ortho substitutions resulted in a loss of activity. Interestingly, while replacement of the C6-(4-methoxybenzylamino) (**118**) with phenylamino resulted in a 6-fold loss of activity, replacement with a 3-chlorophenylamino(**52**) results in a 3-fold improvement in activity. Solution of the purvalanol B-Cdk2 cocrystal structure revealed that the chloro group forms a dipole interaction with Asp 186 as well as potentially strengthening the essential H-bonding interaction between C6 NH and backbone carbonyl of Leu83 located in the kinase hinge region [28]. Similar to the benzylamino substitutent, the phenylamino derivative tolerated meta and para but not ortho substitution. Most potent activity was seen with meta-substituted electron withdrawing substituents although meta amino was also very active presumably due to an H-bond with Asp 186. Multiple kinase sequence alignments demonstrate that this phenyl ring-accommodating pocket shows the most sequence variability suggesting that specificity can be achieved by introducing inhibitor modifications at this site. The general design principle of extending inhibitor contacts into portions of the active site that are poorly conserved across various protein kinases was later supported by structural studies on the class of triarylimidazole p38 Map kinase inhibitors [36]. These structures contain a 4-fluorophenyl moiety that binds in a small hydrophobic groove adjacent to the ATP-binding site. Binding to this groove was shown to be an important specificity determinant by mutation of threonine 106 to a bulky hydrophobic residue (similar to many other kinases) which resulted in loss of activity of the inhibitor [37, 38]. The N9 position faces a small hydrophobic pocket "closed" at the rear by Phe 80. A 10-fold improvement in binding affinity was achieved by replacing the N9-methyl of olomoucine with an isopropyl thereby filling this hydrophobic pocket (olomoucine vs **118**). Recently a purine (**H717**, IC_{50} = 52 nM) with a cyclopentyl group at N9 was cocrystallized with monomeric Cdk2 demonstrating that a slightly larger substitutuent can be tolerated [31].

3.3. Cellular Effects of Trisubstituted Purines Derivatives

Despite being optimized for potent *in vitro* activity and selectivity towards Cdks, are Cdks the functional intra-cellular targets of purine-derived Cdk inhibitors? While the

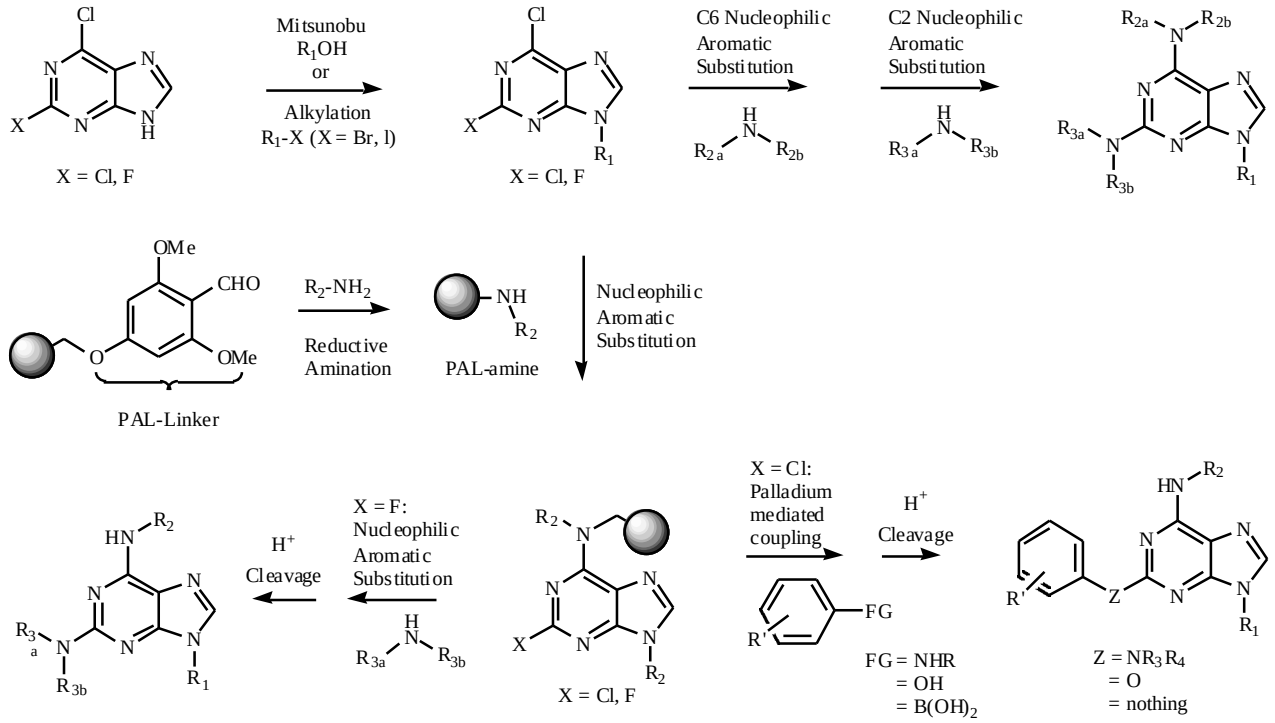

Fig. (8). Methods for the combinatorial synthesis of trisubstituted purines.

Starting from a 2-fluoro or 2,6-dichloropurine scaffold, libraries can be prepared using solution phase chemistry by alkylation at N9 followed by nucleophilic aromatic substitutions at C2 and C6 (A). Solid-phase combinatorial libraries can be prepared by capturingthe alkylated purine from scheme (A) with a resin bound amine followed by C2 substitution using palladium-mediated or direct aminations (B).

answer appears to be yes, there are clearly additional cellular target proteins responsible for purvalanol-induced phenomena. Extensive profiling of the purvalanols against a panel of purified kinases has demonstrated low nanomolar activity only against Cdks (specifically CdkK1/cycB, Cdk2/CycA or E, and Cdk5/p35) (Table **3**). When compounds such as purvalanol A (**60**) and aminopurvalanol (**97**) (Fig. **9**) were tested for their antiproliferative activity against 60 human tumor cell lines at the National Cancer Institute, they exhibited an average IC_{50} values of 2 and 1.8 μM respectively. More detailed cell cycle analysis showed that both compounds induce a G2/Marrest of U937 cells at concentrations between 1 to 10 μM and strongly induce apoptosis at concentrations above 20 μM. The effect of the purvalanols on microtubule architecture and on chromatin condensation were consistent with G2 cell-cycle arrest, based on the low percentage of mitotic cells (< 5 %) seen in treated populations [39]. The phosphorylation of Cdk substrates such as pRB and cyclins A and E were shown to be blocked following treatment of MCF-7 and BP-A31 cells with 10 μM purvalanol A [40]. To evaluate whether aminopurvalanol inhibits Cdk1/cyclin B activity in cultured cells, the level of phosphonucleolin was measured with the phospho-specific antibody TG3. Aminopurvalanol dose-dependently inhibited the phosphorylation of nucleolin following release from a metaphase block with an IC_{50} of 2.2 μM; moreover, aminopurvalanol (**97**) dose-dependently inhibits cell cycle re-entry following serum starvation in CCL39 cells (IC_{50} = 1.5 μM). These results indicate a direct inhibiton of Cdk1/cyclin B by aminopurvalanol at concentrations comparable to those required to inhibit cellular proliferation supporting the idea that Cdk1 is a cellular target.

Despite these clear effects on cell cycle, effective applied cellular concentrations are in the 1 to 10 μM range (approximately 100-fold higher than kinase IC_{50}s measured *in vitro*) making inhibition of other cellular targets a distinct possibility. Another hint that other intracellular targets might be involved comes from the observation that structurally similar and fairly potent Cdk inhibitors such as compound **212** exhibited very different cellular effects. Compound **212** non-specifically induced apoptosis at concentrations as low as 5 μM as assessed by flow cytometric analysis and DNA laddering [39].

3.4. Cellular Targets of Purvalanols

In an effort to learn what other cellular targets may be involved in the mechanism of action of the purvalanols, an affinity chromatography approach was devised to look for interacting proteins. Through an examination of the Cdk2-purvalanol cocrystal structure it was evident that a linker could be installed at the para position of the aniline moiety C6 without disturbing the binding confirmation (Fig. **10**). Affinity chromatography in a series of diverse extract sources ranging from mouse tissues to oocytes and cell lines, resulted in the identification of an expanded set of purvalanol interacting proteins: Cdk 1,2 and cyclin B were isolated from mitotically active extracts, Cdk5/p35 and calmodulin kinase

Table 3. Effect of Purvalanol A, Purvalanol B and Aminopurvalanol A on the Activity of Purified Protein Kinases (IC_{50} Values in nM)

Enzyme	Puvalanol A IC_{50} (nM)	Puvalanol B IC_{50} (nM)	Aminopurvalanol IC_{50} (nM)
Cdk1/cycB	4	6	33
Cdk1/cycB (150 mM ATP)	40	50	ND
Cdk1/cycB (1.5 mM ATP)	500	250	ND
Cdk2/cycA	70	6	33
Cdk2/cycE	35	9	28
Cdk4/cycD1	850	>10’000	ND
Cdk5/p35	75	6	20
Erk1	9’000	3’333	12
Erk2	ND	ND	3.1
c-Raf	ND	ND	>100’000
MAPK	ND	ND	>100’000
c-jun-N-terminal kinase	>1’000	>10’000	ND
PKC-α	>10’000	>100’000	>100’000
PKC-βI	>10’000	>100’000	>100’000
PKC-βII	>10’000	>100’000	>100’000
PKC-γ	>10’000	>100’000	>100’000
PKC-δ	>100’000	>100’000	36
PKC-ε	>100’000	>100’000	>100’000
PKC-ζ	>100’000	>100’000	>100’000
PKC-η	>100’000	>100’000	>100’000
cAMP	9’000	3’800	18
cGMP	>10’000	>100’000	>100’000
Casein kinase 1	>3’333	>3’333	3
Casein kinase 2	>10’000	>10’000	>100’000
GSK3-β	>10’000	>10’000	ND
Insulin-receptor kinase	5’000	2’200	4.4
Raf kinase	>1’000	>10’000	ND
v-abl	>10’000	>100’000	ND
Cdc28 (S. cerevisiae)	80	1’200	ND
Her-1	6’300	5’800	7’200
Her-2	15’200	24’200	10’600
IGF-1R	30’000	6’700	7’900
KDR	4’275	9’000	6’300
FGFR-1	15’000	21’000	7’200
c-kit	16’500	25’500	9’500
c-Met	45’500	65’500	14’000

For experimental details see Table 1.

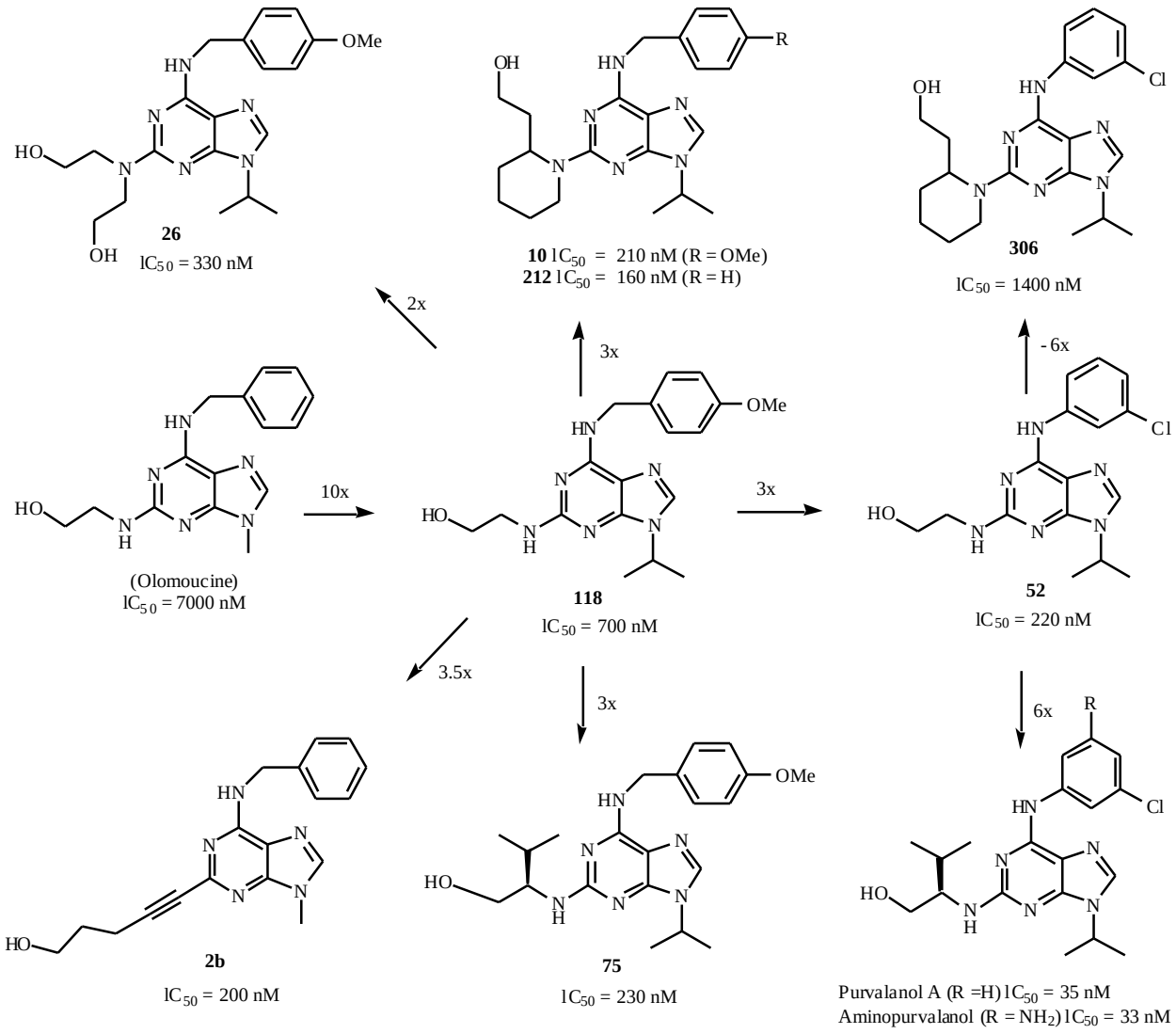

Fig. (9). Representative compounds illustrating structure-activity relationships derived from modifications to the 2, 6, and 9 positions of the purine ring (IC_{50} values against Cdk2/cyclin A are shown).

from pig brain or neuronal cell lines, Erk1 and Erk 2 from five different cell lines (CCL39, PC12, HBL100, MCF-7, and Jurkats), and focal adhesion kinase (FAK) and p90RSK from mouse brain (unpublished result) [41]. In order to assure that these interactions were specific to the active purvalanol pharmacophore, control matrices were prepared where the essential C6 hydrogen bond donor was methylated. This modification results in a complete loss of kinase inhibitory activity. Aminopurvalanol inhibited bacterially expressed Erk1 and Erk 2 with IC_{50}s in the low micromolar range which is approximately 100-fold higher than the nanomolar Cdk inhibitory activities. In order to assess whether there was a correlation between *in vitro* IC_{50}s measured on purified Erk1,2 versus functional intracellular inhibition, the ability of aminopurvalanol to functionally block Elk1 transcriptional activity was measured. Aminopurvalanol dose-dependently inhibited Erk1/2 pathway with an IC_{50} of 4 μM and inhibited epidermal growth factor (EGF)-induced hepatocyte spreading at 1 μM [42]. Interestingly, aminopurvalanol exhibited a 10-fold higher IC_{50} against the Cdk1/cyclin B (IC_{50} = 350 nM) purified specifically from the cell lines used to study the MAPK pathway (CCL9, fibroblasts) than on the starfish Cdk1/cyclin B or baculovirally expressed Cdk2/cyclin A[23]. Taken together these results suggest that the purvalanols exert their antiproliferative effects through combined action on both the MAPK pathway and Cdks.

CONCLUSIONS AND PERSPECTIVES

In conclusion potent and selective inhibitors of cyclin-dependent kinases have been developed which contain the phenylaminopyrimidine pharmacophore as exemplified by CGP60474 and the purvalanols. The antiproliferative activity of CGP60474 is consistent with its ability to inhibit Cdk1/2 and it appears to be exhibit enhanced cytotoxicity towards cells with defective G1/S checkpoints. CGP60474 exhibited

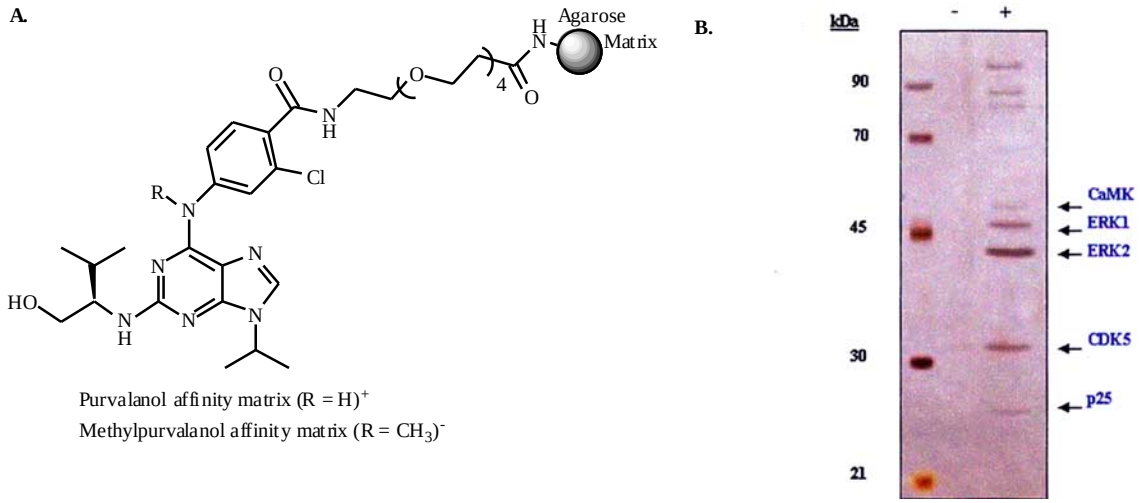

Fig. (10). Affinity chromatography approach for identification of intracellular targets of purvalanol.

Structure of immobilized purvalanol and N6-methylated control resin (A). Example of proteins retained from mouse brain extracts from purvalanol (+) and methylpurvalanol (-) affinity matrix. Proteins identified by excission of bands followed by mass spectrometry.

antiproliferative IC_{50}s of less than 100 nM against a large variety of cancer cell lines. The trisubstiuted purvalanols exhibit a similar low nanomolar IC_{50} against Cdk1 / 2 but are considerably less antiproliferative with IC_{50}s in the single digit micromolar range against a variety of cell lines. This is unlikely to result from poorer cellular permeability of the purine derived Cdk inhibitors as compounds with low nanomolar cellular IC_{50}s have been developed targeting other kinases. One possibility is that additional cellular targets for the phenylaminopyrimidines such as CGP60474 remain to be identified. In addition while optimization work was ongoing on these two inhibitor classes, Cdk7, 8, 9 and 10 were cloned and implicated in the control of transciption. The extent of involvement of these highly homologous kinases in the mechanism of action of the purvalanols and CGP60474 remains to be determined. It is likely that the development of successful therapeutics targeting Cdks will require further elucidation of the complexities of cyclic dependent kinase regulation in the context are partially selective antagonists.

ABBREVIATIONS

ATP	=	Adenosine trisphosphate
Cdk	=	Cyclin-dependent kinase
IC_{50}	=	Concentration causing 50% inhibition
PAP	=	Phenyl-amino-pyrimidines
RB	=	Retinoblastoma protein

REFERENCES

[1] Gould, K.L. *Front. Mol. Biol.*, **2000**, *29*, 277.

[2] Sherr, C.J.; Roberts, J.M. *Genes Dev.*, **1999**, *13*, 1501.

[3] Sherr, C.J. *Science*, **1996**, *274*, 1672.

[4] Sherr, C.J. *Cancer Res.*, **2000**, *60*, 3689.

[5] Fabbro, D.; Ruetz, S.; Buchdunger, E.; Cowan-Jacob, S.; Fendrich, G.; Liebetanz, J.; Mestan, J.; O'Reilly, T.; Traxler, P.; Chaudhuri, B.; Fretz, H.; Zimmermann, J.; Meyer, T.; Caravatti, G.; Furet, P.; Manley, P. *Pharmacol. Ther.*, **2002**, 93.

[6] Hartwell, L.H.; Kastan, M.B. *Science*, **1994**, *266*, 1821.

[7] Walworth, N.C. *Curr. Opin. Cell Biol.*, **2000**, *12*, 697.

[8] Harper, J.W.; Adams, P.D. *Chem. Rev.* **2001**, *101*, 2511.

[9] Nigg, E.A. *Nat. Rev. Mol. Cell Biol.*, **2001**, *2*, 21.

[10] Harbour, J.W.; Dean, D.C. *Nat. Cell Biol.*, **2000**, *2*, E65.

[11] Kaelin, W.G. *Bioassays*, **1999**, *21*, 950.

[12] Senderowicz, A.M.; Sausville, E.A. *J. Natl. Cancer Inst.*, **2000**, *92*, 376.

[13] Senderowicz, A.M. *Oncogene*, **2000**, *19*, 6600.

[14] Mani, S.; Wang, C.; Wu, K.; Francis, R.; Pestell, R. *Expert. Opin. Investig. Drugs*, **2000**, *9*, 1849.

[15] Sausville, E.A.; Johnson, J.; Alley, M.; Zaharevitz, D.; Senderowicz, A.M. *Ann. N Y Acad. Sci.*, **2000**, *910*, 207; discussion 221.

[16] Meijer, L. *Drug Resist. Update*, **2000**, *3*, 83.

[17] Zimmermann, J.; Caravatti, G.; Mett, H.; Meyer, T.; Muller, M.; Lydon, N.B.; Fabbro, D. *Arch. Pharm.*, **1996**, *329*, 371.

[18] Zimmermann, J.; Buchdunger, E.; Mett, H.; Meyer, T.; Lydon, N.B. *Bioorg. Med. Chem. Lett.*, **1997**, *7*, 187.

[19] Krek, W.; DeCaprio, J. A. *Meth. Enzymology*, **1995**, *254*, 114.

[20] Imbach, P.; Capraro, H.G.; Furet, P.; Mett, H.; Meyer, T.; Zimmermann, J. *Bioorg. Med. Chem. Lett.* **1999**, *9*, 91.

[21] Glab, N.; Labidid, B.; Qin, L.X.; Trehin, C.; Bergounioux, C.; Meijer, L. *FEBS Lett.*, **1994**, *353*, 207.

[22] Schutte, B.; Nieland, L.; van Engeland, M.; Henfling, M.E.; Meijer, L.; Ramaekers, F.C. *Exp. Cell Res.*, **1997**, *236*, 4.

[23] Krucher, N.A.; Meijer, L.; Roberts, M.H. *Cell. Mol. Neurobiol.*, **1997**, *17*, 495.

[24] Schulze-Gahmen, U.; Brandsen, J.; Jones, H.D.; Morgan, D.O.; Meijer, L.; Vesely, J.; Kim S.H. *Proteins: Struct. Funct. Genet.*, **1995**, *22*, 378.

[25] Legraverend, M.; Ludwig, O.; Bisagni, E.; Leclerc, S.; Meijer, L.; Giocanti, N.; Sadri, R.; Favaudon, V. *Bioorg. Med. Chem*., **1999**, *7*, 1281.

[26] Gray, N.S.; Detivaud, L.; Doerig, C.; Meijer, L. *Curr. Med. Chem.*, **1999**, *6*, 859.

[27] Sielecki, T.M.; Boylan, J.F.; Benfield, P.A.; Trainor, G.L.: *J. Med. Chem.*, **2000**, *3*, 1.

[28] Meijer, L.; Borgne, A.; Mulner, O.; Chong, J. P.; Blow, J.J.; Inagaki, N.; Inagaki, M.; Delcros, J.G.; Moulinoux, J.P. *Eur. J. Biochem*., **1997**, *243*, 527.

[29] Gray, N.S.; Wodicka, L.; Thunnissen, A.M.; Norman, T.C.; Kwon, S.; Espinoza, F.H.; Morgan, D.O.; Barnes, G.; LeClerc, S.; Meijer, L.; Kim, S.H.; Lockhart, D.; Schultz, P.G.: *Science*, **1998**, *281*, 533.

[30] Brooks, E.E.; Gray, N.S.; Joly, A.; Kerwar, S.S.; Lum, R.; Mackman. R.L.; Norman, T.C.; Rosete, J.; Rowe, M.; Schow, S.R; Schultz, P.G; Wang, X.; Wick, M.M.; Shiffman, D. *J. Biol. Chem.*, **1997**, *272*, 29207.

[31] Dreyer, M.K.; Borcherding, D.R.; Dumont, J.A.; Peet, N.P.; Tsay, J.T.; Wright, P.S.; Bitonti, A.J.; Shen, J.; Kim, S.H. *J. Med. Chem.*, **2001**, *44*, 524.

[32] Arris, C.E.; Boyle, F.T.; Calvert, A.; Curtin, N.J.; Endicott, J.A.; Garman, E.F.; Gibson, A.E.; Golding, B.T.; Grant, S.; Griffin, R.J.; Jewsbury, P.; Johnson, L.N.; Lawrie, A.M.; Newell, D.R.; Noble, M.E.; Sausville, E.A.; Schultz, R.; Yu, W. *J. Med. Chem.*, **2000**, *43*, 2797.

[33] Noble. M.E.; Endicott, J.A. *Pharmacol. Therapeutics*, **1999**, *82*, 269.

[34] Ding, S.; Gray, N.S.; Ding, Q.; Wu, X.; Schultz, P.G. *J. Comb. Chem*., **2002**, *4*, 183.

[35] Ding, S.; Gray, N.S.; Ding, Q.; Schultz, P.G. *J. Org. Chem*., **2001**, *66*, 8273.

[36] Tong, L.; Pav, S.; White, D.M.; Rogers, S.; Crane, K.M.; Cywin, C.L.; Brown, M.L.; Pargellis, C.A. *Nat. Struct. Biol.*, **1997**, *4*, 311.

[37] Eyers, P.A.; Craxton, M.; Morrice, N.; Cohen, P.; Goedert, M. *Chem. Biol.*, **1998**, *5*, 321.

[38] Gum, R.J.; McLaughlin, M.M.; Kumar, S.; Wang, Z.; Bower, M. J.; Lee, J.C.; Adams, J.L.; Livi, G.P.; Goldsmith, E.J.; Young, P.R. *J. Biol. Chem.*, **1998**, *273*, 15605.

[39] Chang, Y.T.; Gray, N.S.; Rosania, G.R.; Sutherlin, D.P.; Kwon, S.; Norman, T.C.; Sarohia, R.; Leost, M.; Meijer, L.; Schultz, P.G. *Chem. Biol.*, **1999**, *6*, 361.

[40] Villerbu, N.; Gaben, A.M.; Redeuilh, G.; Mester, J. *Int. J. Cancer*, **2002**, *97*, 761.

[41] Knockaert, M.; Gray, N.S.; Damiens, E.; Chang, Y.T.; Grellier, P.; Grant, K.; Fergusson, D.; Mottram, J.; Soete, M.; Dubremetz, J.F.; Le Roch, K.; Doerig, C.; Schultz, P.; Meijer, L. *Chem. Biol.*, **2000**, *7*, 411.

[42] Knockaert, M.; Lenormand, P.; Baffet, G.; Gray, N.S., Schultz, P.G.; Poussegur, J.; Meijer, L. *Oncogene*, **2002**, in press

[43] Furet, P.; Zimmermann, J.; Capraro, H.G.; Meyer. T.; Imbach, P. *J. Comput. Aided Mol. Des.*, **2001**, *14*, 403.

[44] Soni, R.; O'Reilly, T.; Furet, P.; Muller, L.; Stephan, C.; Zumstein-Mecker, S.; Fretz, H.; Fabbro, D.; Chaudhuri, B. *J. Natl. Cancer Inst,*. **2001**, *93*, 436.

[45] Idziorek, T.; Estaquier, J.; De Bels, F. *J. Immunol. Methods*, **1995**, *185*, 249.